# SIMULATION OF CASTING SOLIDIFICATION PARAMETERS IN METALLIC MOULD

**Ayad M. Takhakh**
Mechanical Engineering Department, University of Al-Nahrain, Baghdad-Iraq
**Akeel D. Subhi**
Department of Production Engineering and Metallurgy, University of Technology, Baghdad-Iraq

## ABSTRACT

In this work, numerical method approach has been used to simulate the solidification parameters of an eutectic aluminum-silicon alloy in chilled metallic mould with copper. The approach is based on the solution of heat flow equations of the casting and mould. In addition, the latent heat is treated as a boundary condition between the liquid and solid phase. The results showed that different behaviors of solidification parameters are obtained along the casting. Furthermore, the simulation approach of solidification parameters in conjunction with the microstructure indicated that it is possible, to a large degree, giving a knowledge about the microstructural features for any alloy system.

## الخلاصة

تم في هذا البحث استخدام الطريقة الرقمية في محاكاة متغيرات التجمد لسبيكة الالمنيوم–سليكون الايوتكتيكية في قالب معدني مزود بمصقع من النحاس. اذ تستند الطريقة المستخدمة على حل معادلات انسياب الحرارة للمسبوكة والقالب. اضافة لذلك فقد تم اعتماد الحرارة الكامنة كظرف للحد الفاصل بين السائل والصلب. وقد اوضحت النتائج وجود اختلاف في سلوك متغيرات التجمد على طول المسبوكة. علاوة على ذلك فقد تم التوصل من خلال الربط ما بين محاكاة متغيرات التجمد والبنية المجهرية الى امكانية الاستفادة من نتائج المحاكاة لهذه المتغيرات للتنبا بالسمات المجهرية الى حد كبير ولاي نظام سبائكي.

## KEY WORDS

Solidification parameters, simulation, metallic mould, aluminum-silicon alloy, microstructure

## INTRODUCTION

Casting, one of the important manufacturing processes, has been used more widely in industry **(Schey 2000)**. It is a very economic method of forming a component and in the same time a complicated process involving control the metallurgical and mechanical aspects **(Metals Handbook 1998)**. The properties of solidified metal or alloy are dependent not just on composition but also on grain size and the shape and distribution of phases **(Metals Handbook 1998 and Campbell 2004)**. These factors can be controlled and modified through controlling the solidification process. The cooling rate, temperature gradient, and local solidification time, which are the solidification parameters, govern the microstructure which in turn control the mechanical properties **(Campbell 2004)**.

The simulation of solidification has received increased attention as the computer revolution has matured. Simulation will be very important tool to optimize the casting process, to shorten the lead time, to assure the quantity, and to improve the mechanical properties of castings **(Kurz and Fisher 1986)**. A wide range of efforts is being used to simulate the solidification and microstructure evolution. These include finite element method (FEM) **(Masters et al. 1997 and Guillemot et al. 2004)**, finite difference method (FDM) **(Palmer and Games dos Santos 1998 and Lu 2002)**, finite volume method (FVM) **(Warran et al. 2002 and Lewis 2004)**, cellular automation method (CAM) **(Varam et al. 2001 and Qingyan et al. 2005)**, etc.

The main research objective is to simulate the solidification parameters of Al-12%Si alloy casted in chilled metallic mould using a numerical method approach. The simulated solidification parameters are coupled with microstructure that evolved during solidification in order to develop a modified approach.

## MODEL ASSUMPTIONS

The filling of metallic mould with molten metal of eutectic Al-Si alloy is assumed to be instantaneous in this work. It is also assumed that no convection in the molten metal of eutectic alloy. This is related to the redistribution of solute that takes place within the boundary layer, in which this layer is smaller than the momentum boundary layer resulting from the molten metal flow **(Flemings 1974)**. Thermal conductivity and density are considered to be variable with the temperature. While the thermophysical properties of the mould are considered to be constant.

## MATHEMATICAL MODEL

Macro-Micro model is built to simulate the solidification of the eutectic Al-12%Si alloy system. The eutectic Al-12%Si alloy was prepared using pure aluminum, Al-22%Si master alloy as starting materials. The chemical composition of pure aluminum, master alloy and prepared Al-12%Si alloy are illustrated in **Table I**. After adjusting the chemical composition, the molten of Al-12%Si alloy was poured in a rectangular metallic mould made from stainless steel and chilled with copper (**Fig. 1**). The simulation of solidification requires the application of heat transfer equations and also some special technique to simulate the latent heat release. For the molten metal that undergoing from solidification, the latent heat is a new factor which needs to be incorporated into the simulation program. In this paper, the solidification range was assumed to be 10 $^{\circ}$C (565 – 575 $^{\circ}$C).

The liquid and solid phases were modeled separately in which the latent heat is treated as a boundary condition. The initial boundary conditions can be expressed as:

At t=0; $T_{mold}$= 30 $^{\circ}$C

$T_{chill}$= 30 °C
$T_{air}$ = 30 °C

While the boundary conditions can be expressed as:
(a)- At the internal point, the general heat conduction equation in the casting for liquid phase is:

$$k_L\left(\frac{\partial^2 T}{\partial X^2}+\frac{\partial^2 T}{\partial Y^2}+\frac{\partial^2 T}{\partial Z^2}\right)=\rho_L C_{PL}\frac{\partial T}{\partial t} \qquad (1)$$

While for solid phase, the general heat conduction equation will be

$$k_S\left(\frac{\partial^2 T}{\partial X^2}+\frac{\partial^2 T}{\partial Y^2}+\frac{\partial^2 T}{\partial Z^2}\right)=\rho_S C_{PS}\frac{\partial T}{\partial t} \qquad (2)$$

- For mushy zone, the general heat conduction equation is

$$k_m\left(\frac{\partial^2 T}{\partial X^2}+\frac{\partial^2 T}{\partial Y^2}+\frac{\partial^2 T}{\partial Z^2}\right)+\rho L\frac{\partial f_s}{\partial t}=\rho_m C_{Pm}\frac{\partial T}{\partial t} \qquad (3)$$

(b)- At the mould/air interface

$$Q = h_{air}(T_{air}-T_{mold}) \qquad (4)$$

At the external surface, a constant heat transfer coefficient is taken to be 15 $W/m^2.K$ for mould/air interface region **(Baily 1988)**.

In the solidification of a given alloy, the amount of liberated latent heat is considered to be proportional to the fraction of solid, which is calculated using the lever rule **(Rappaz 1989)**. All equations are solved using finite difference method to determine the temperatures history for casting at each determined node.

The energy equation that related to heat conduction in metallic mould can be expressed as:

$$\rho_m C_{pm}\frac{\partial T_m}{\partial t} = k_m\left[\frac{\partial^2 T}{\partial X^2}+\frac{\partial^2 T}{\partial Y^2}+\frac{\partial^2 T}{\partial Z^2}\right] \qquad (5)$$

where the subscript m represents the mould. The above equations must be solved with appropriate initial boundary conditions.

Image processing was performed using image J program. In this program, the microstructural picture of all specimens that sectioned from the Al-12%Si alloy casting at different positions was inserted to the program separately and processing was achieved.

Fisher and Kurz equation **(Fisher and Kurz 1980)** was used to calculate eutectic spacing (λ). This equation can be expressed as

$$\lambda = \frac{\lambda_e+\lambda_b}{2} \qquad (6)$$

where $\lambda_e$ is the spacing at the extremity and $\lambda_b$ is the branching spacing in which the range of stable eutectic growth is located between them.

## RESULTS AND DISCUSSION

The cooling curve of Al-12%Si alloy at different positions along the casting can be shown in **Fig. 2**. It is clear from this figure that the solidification time is very short near the chill/cast interface and then increases until reaching a specified distance of 20 mm. Without any doubt, this distance is a transition point in which the solidification time over it has approximately a constant value (0.584 s). The ascription of differences in cooling curve behavior at different positions along the casting is related to the differences in cooling rate. As a result of using copper chill, the cooling rate will be very high at the chill/cast interface region and then decreases with ascending until reaching a specified distance of 20 mm as shown in **Fig. 3**. The constancy in cooling rate (53.093 $^{\circ}$C/s) can be shown clearly beyond a distance of 20 mm. In addition, **Fig. 3** also shows that the cooling rate at the casting corner is very high compared with that along the casting center. This is related to the mould wall which acts as a chill. This accompanied with the copper chill that already existed and conducted with the mould in comparison with that along the casting center which is affected only by the copper chill. This increasing in the cooling rate leads to modify the microstructure of Al-12%Si alloy which in turns raise the mechanical properties.

The relationship between temperature gradient and distance at different positions along the casting can be shown in **Fig. 4**. The important notice that can be recognized form this figure is that the temperature gradient is high in the region that conducted with the copper chill. This increasing in the temperature gradient does not remain the same as that in the early stage of solidification in which the distance of 20 mm that measured from the chill/cast interface is a transition point where the temperature gradient decreases beyond it. **Fig. 4** also shows that the temperature gradient laterally is too high especially at the mould wall compared with that at the casting center. This is because the mould wall acts as a chill during solidification. Because of the small thickness of mould wall used compared with the molten metal volume, this makes the mould wall unable to act as a chill through all stages of solidification. Therefore, decreases in temperature gradient laterally can be recognized obviously with departing from the mould wall toward the casting center.

Some directional solidification can be observed in the early stage of solidification as shown in **Fig. 5** which represents the relationship between local solidification time and distance. This can be demonstrated by the linear relationship between local solidification time ($t_s$) and distance (d) until reaching a specified distance of 20 mm according to the following relationship which can be expressed as

$$t_s = 0.033d - 0.019 \qquad (7)$$

Beyond this distance, constancy in solidification time can be recognized until completing the solidification. This means that chill effect is limited up to distance of 20 mm measured from the chill/cast interface and beyond this; no effect of chill has been occurred.

The effect of changes that occurred in solidification parameters along Al-12%Si alloy casting as a result of using copper chill was reflected on the microstructural features as shown in **Fig. 6**. It is important to recognize that flake silicon phase with different degrees of modification are presented along the Al-12%Si alloy casting. Several investigators studied the mechanism of modification in Al-Si alloys either quench or chemical **(Kobayashi and Hogan 1985)**. Because of using a copper chill, the modification of eutectic silicon phase related certainly to chill effect. As mentioned elsewhere, quench modification was originally attributed to the repeated nucleation of the eutectic silicon phase at a reduced temperature **(Metals Handbook 1998)**. Near the chill/cast interface region, as shown in **Fig. 6a**, the greatest modification in flake silicon phase can be recognized. This is related to high cooling rate in this region that reaches to 256.676 °C/s. Moderate modification can be observed in flake silicon phase with departing from the chill/cast interface region as shown in **Figs. 6b and c**. This is related to decrease the chill effect. The depletion of chill effect at distance of 20 mm, as shown in **Fig. 6d**, and over it makes the size and morphology of flake silicon phase slightly changed, as shown in **Figs. 6e-g**.

From this, the magnitude of solidification parameters at a given point along the Al-12%Si alloy casting has a strong role on determining the eutectic spacing (λ) and morphology of silicon phase. The predominant morphology of silicon phase, as explained above, is flake. As represented in **Table II**, which is essence of the results of the present work, no changes in eutectic spacing (λ) can be observed at and beyond a specified magnitude of solidification parameters that corresponding to (R=53.696 °C/s, G=14.987 °C/mm, $t_s$=0.577 s) and distance (20 mm). Of course, this is related to depleting the chill effect. This means that no modification in flake silicon can be observed at distance of 20 mm and beyond it. The most important result that can be concluded from **Table II** is that the relationship between the solidification parameters and microstructural features of Al-12%Si alloy casting can be used to predict the microstructural features for any other alloy system after determination the casting conditions, thermal properties of the casting and the mould, and system constituents used.

## CONCLUSIONS

The prediction of solidification parameters using numerical method approach has been developed. The results showed that different behaviors of solidification parameters are obtained along the chilled Al-12%Si alloy casting using copper. The results also showed that the distance of 20 mm measured from the chill/cast interface is a transition point in which constancy, to a large degree, in the solidification parameters is produced. Furthermore, the numerical approach has been extended to include microstructural features. From the simulation of solidification parameters-microstructure relationship, one can predict the microstructual features for any other alloy system.

## REFRENCES

-Baily, C., “Computational Modeling of Mold Design in Lead Ingot Casting", Modeling of Casting, Welding and Advanced Solidification Processes, Vol. VIII (1988) 827.

-Campbell, J., “Castings”, Elsevier Butterworth-Heinemann (London) 2004.

-Fisher, D.J. and Kurz, W., “A Theory of Branching Limited Growth of Irregular Eutectics”, Acta Metallurgica, 28 (1980) 777.

-Flemings, M.C.," Solidification Processing", McGraw-Hill, Inc. (New York) 1974.

-Guillemot, G. et al., “A New Cellular Automation-Finite Element Coupling Scheme for Alloy Solidification”, Modeling Simul. Mater. Sci. Eng., 12 (2004) 545.

-Kobayashi, K.F. and Hogan, L.M., “The crystal Growth of Silicon in Al-Si Alloys”, J. Mater. Sci., 20 (1985) 1961.

-Kurz, W. and Fisher, D.J., “Fundamentals of Solidification”, Trans Tech Publication Ltd (Switzerland) 1986.

-Lewis, D., “Phase Field Models for Eutectic Solidification”, JOM, (2004) 34.

Lu, Y., “Convection Effects in Three-Dimensional Dendritic Growth”, ASME International Mechanical Congress and Exposition, (2002) 17.

-Masters, I. et al., “Finite Element Analysis of Solidification Using Object-Oriental and Parallel Techniques”, International Journal for Numerical Methods Engineering, 40 (1997) 2891.

-Metals Handbook, Vol. 15, “Casting”, American Society for Metals, Metals Park, Ohio, 1998.

-Palmer, W. and Games dos Santos, R., “Numerical Analysis of Steel Solidification Using Finite Difference Method and Finite Element Method”, Modeling of Casting, Welding and Advanced Solidification Processes VIII (1998) 1063.

-Qingyan et al., “Modeling of Dendritic Structure During Solidification Process Base on Cellular Automation Model”, Mater. Sci. Forum, 475-497 (2005) 3137.

-Rappaz, M., “Modeling of Microstructure Formation in Solidification Process”, Intern. Mater. Reviews, 34 (1989) 93.

-Schey, J.A., “Introduction to Manufacturing Processes”, McGraw-Hill Higher Education (Singapore) 2000.

-Varam, M.R. et al., “Cellular Automation Simulation of Microstructure Evolution During Austenitic Decomposition Under Continuous Cooling Conditions”, Bull. Mater. Sci., 24 (2001) 305.

-Warran, W.J. et al., “Phase Field Simulation of Solidification”, Annual Review of Materials Research, 32 (2002) 163.

**Greek and Latin Symbols**

| **Symbols** | **Definition** | **unit** |
|---|---|---|
| $\rho$ | Density | $kg/m^3$ |
| $\lambda$ | Eutectic spacing | mm |
| $\lambda_b$ | Eutectic spacing at which branching occurs | mm |
| $\lambda_e$ | Eutectic spacing at the extremity | mm |
| T | Temperature | $^{\circ}C$ |
| G | Temperature gradient | $^{\circ}C/mm$ |
| R | Cooling rate | $^{\circ}C/sec$ |
| $C_p$ | Specific heat | J/kg.K |
| K | Thermal conductivity | W/m.K |
| L | Latent heat | J/kg |
| h | Heat transfer coefficient | $W/m^2.K$ |
| $t_s$ | Local solidification time | sec |
| Q | Heat flux | $W/m^2$ |
| x,y,z | Cartesian coordinates | |

| | | |
|---|---|---|
| f | Phase fraction | |

| Elements (Wt.%) | Si | Fe | Pb | Cu | Mn | Cr | Ni | Ti | Al |
|---|---|---|---|---|---|---|---|---|---|
| Al | 0.119 | 0.276 | 0.001 | 0.005 | 0.004 | 0.001 | 0.001 | 0.005 | Rem. |
| Al-22%Si alloy | 22.30 | 0.190 | 0.011 | 0.020 | 0.157 | 0.006 | 0.006 | 0.043 | Rem. |
| Al-12%Si alloy | 12.30 | 0.220 | 0.014 | 0.018 | 0.151 | 0.004 | 0.005 | 0.034 | Rem. |

**Table I** Chemical composition of pure aluminum, master alloy and prepared Al-12%Si alloy.

**Table II** The eutectic spacing and degree of modification as a function to the solidification parameters.

| **Distance from the chill/cast interface (mm)** | **Microstructural features** | | **Solidification parameters** | | |
|---|---|---|---|---|---|
| | Eutectic spacing (λ) (μm) | Degree of modification | Cooling rate, (R) (°C/s) | Temperature gradient,(G) (°C/mm) | Local solidification time, ($t_s$) (sec) |
| At interface | - | Excellent | 1501.640 | 51.509 | 0.021 |
| 5 | 5.6 | Potent | 256.676 | 28.569 | 0.121 |
| 10 | 8.5 | Moderate | 92.540 | 20.345 | 0.353 |
| 15 | 9.1 | Moderate | 59.816 | 17.882 | 0.518 |
| 20 | 12.5 | No modification | 53.696 | 14.987 | 0.577 |

| | | | | | |
|---|---|---|---|---|---|
| 35 | 12.6 | No modification | 53.093 | 14.631 | 0.584 |
| 50 | 12.6 | No modification | 53.093 | 14.631 | 0.584 |
| 65 | 12.7 | No modification | 53.093 | 14.631 | 0.584 |

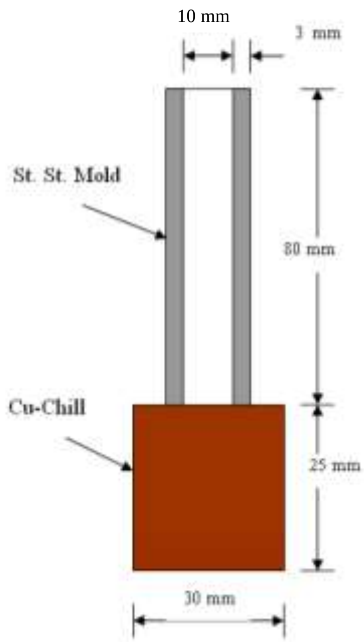


**Fig. 1** Rectangular metallic mould chilled with copper.

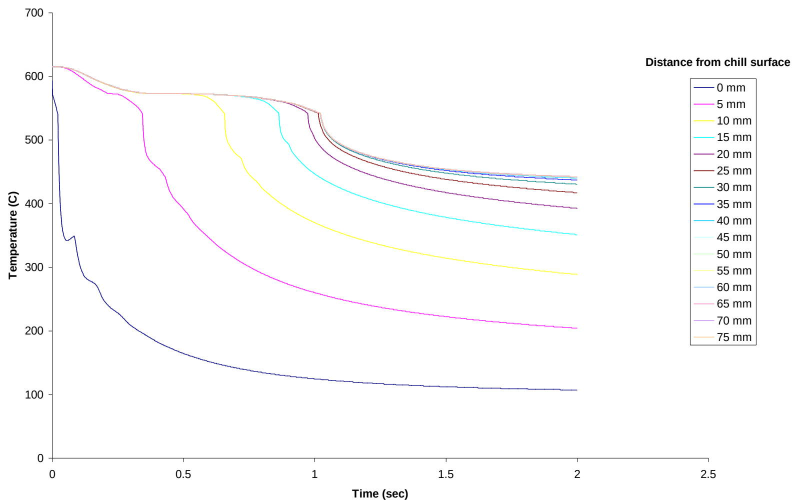


**Fig. 2** The cooling curves at different positions along the casting of Al-12%Si alloy.

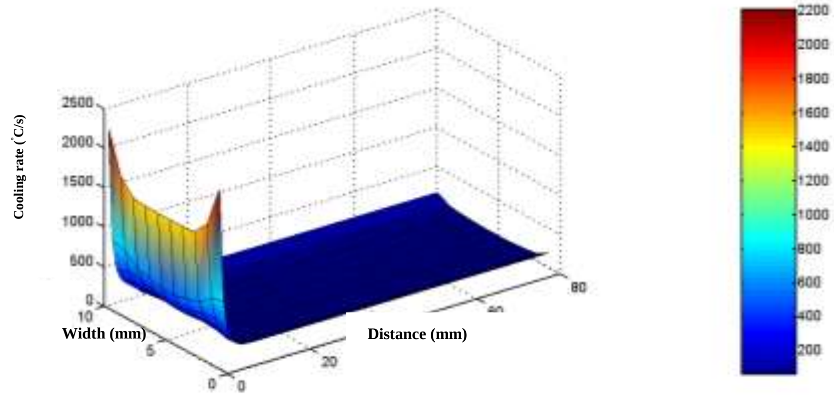


**Fig. 3** The relationship between cooling rate distribution and distance along the casting of Al-12%Si alloy.

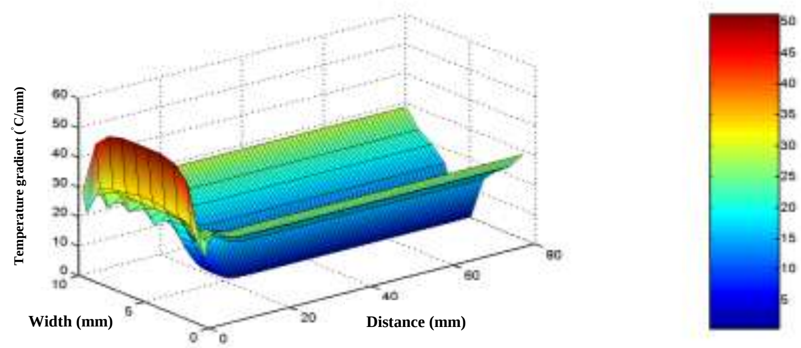


**Fig. 4** The relationship between temperature gradient distribution and distance along the casting of Al-12%Si alloy.

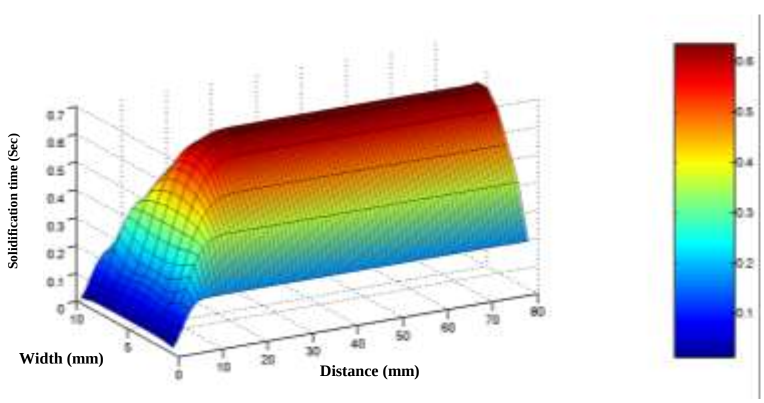


**Fig. 5** The relationship between local solidification time distribution and distance along the casting of Al-12%Si alloy.

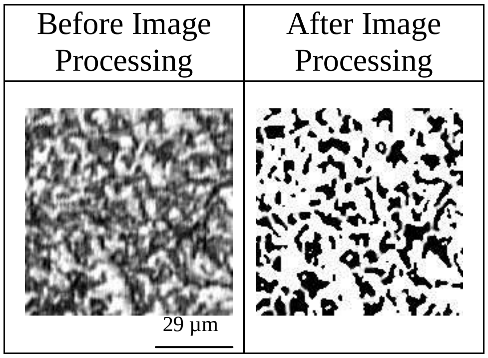
Before Image Processing
After Image Processing
29 µm

(a)

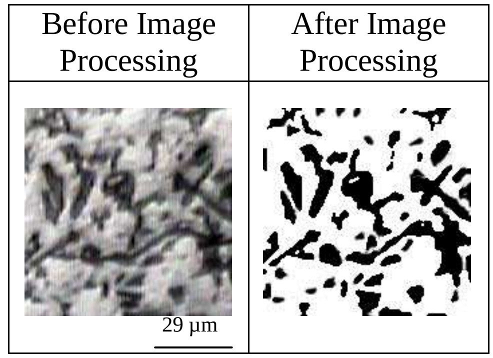
Before Image Processing
After Image Processing
29 µm

(b)

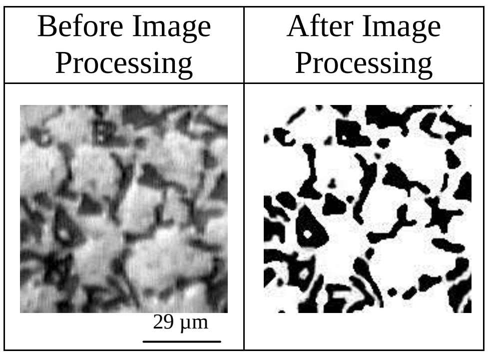
Before Image Processing
After Image Processing
29 µm

(c)

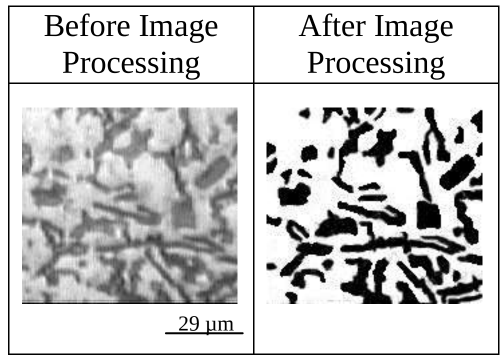
Before Image Processing
After Image Processing
29 µm

(d)

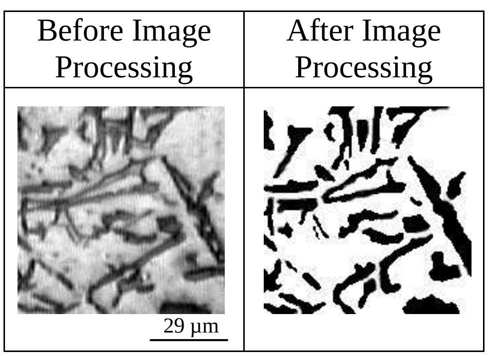
Before Image Processing
After Image Processing
29 µm

(e)

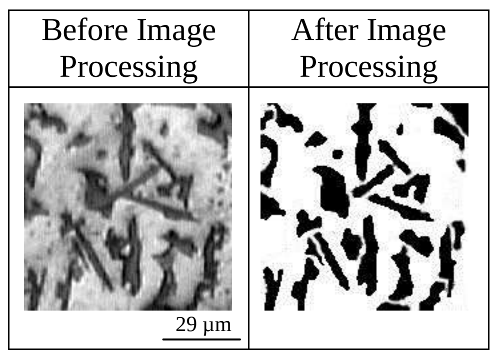
Before Image Processing
After Image Processing
29 µm

(f)

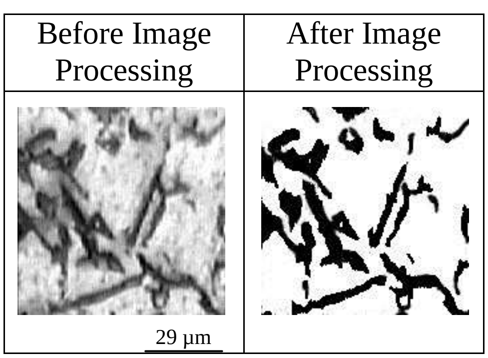
Before Image Processing
After Image Processing
29 µm

(g)

**Fig. 6** Microstructure of Al-12%Si alloy casting before and after image processing at different positions measured from the chill/cast interface; a=5mm, b=10mm, c=15mm, d=20mm, e=35mm, f=50mm, g=65mm. Optical microscopy; etched with 0.5%Vol. hydrofluoric acid.